

# Gauge covariance of the gap equation: from the rainbow truncation to gauge symmetry constraints

Bruno El-Bennich<sup>1</sup> 

<sup>1</sup> Departamento de Física, Universidade Federal de São Paulo, Rua São Nicolau 210, Diadema, 09913-030 São Paulo, Brazil; bennich@unifesp.br

<sup>2</sup> Instituto de Física Teórica, Universidade Estadual Paulista, Rua Dr. Bento Teobaldo Ferraz 271, 01140-070 São Paulo, São Paulo, Brazil

**Abstract:** The gauge covariance of the quark gap equation is compared for three quark-gluon vertices: the bare vertex, a Ball-Chiu like vertex constrained by the corresponding Slavnov-Taylor identity, and a full vertex including the transverse components derived from transverse Slavnov-Taylor identities. The covariance properties are verified with the chiral quark condensate and the pion decay constant in the chiral limit.

**Keywords:** Quantum Chromodynamics, Light Quarks, Gauge Covariance, Gap Equation, Dyson-Schwinger Equation, Dynamical Chiral Symmetry Breaking

## 1. Symmetries: when to break, when to preserve

One of the great achievements of the past decades in hadron physics has been the demonstration that *dynamical chiral symmetry breaking* is overwhelmingly responsible for the masses of nucleons and atoms [1,2]. Indeed, while the Brout-Englert-Higgs mechanism is the source of explicit chiral symmetry breaking, expressed by current-quark mass terms in the Standard Model Lagrangian, the symmetry breaking due to gluon dynamics is incomparably more efficient in generating the mass scales we observe in nuclear physics. This is possible because in describing strong interactions with a relativistic quantum field theory, namely Quantum Chromodynamics (QCD), we also deal with the implicit Einstein formula  $E = mc^2$ . In other words, most of the visible mass we observe is due to radiation energy. It seems as though *Nature* is telling us in a twisted manner that perfect symmetry is not always what she aims at.

On the other hand, gauge symmetry and its preservation have been the *leitmotif* in developing relativistic quantum field theories during the past century and are still guiding physicists in the pursuit of Standard Model extensions. This is a natural demand for any theory, as one can redefine the fields and particles by a gauge transformation in such a way that the physical laws remain the same. Simply put, gauge symmetries are nothing else but redundant degrees of freedom or an over-complete description of a physical system. One may do whatever one wishes with the superfluous degrees of freedom, as the physics of given system remains the same and any measurable quantities cannot depend on how we choose them. This is commonly called gauge invariance and is also intimately related to the renormalizability of a quantum field theory. For instance, the Ward-Green-Takahashi identity (WGTI) [3–5] that describes current conservation in Quantum Electrodynamics (QED) implies that the wave function renormalization of the electron and its vertex renormalization constant are equal. This identity is crucial to the cancellation of the ultraviolet divergences that occur in loop calculations to all orders in perturbation theory.

Now, while we insist on gauge symmetry to be preserved at all times, we still have to deal with the freedom to redefine fermion and gauge fields. The consequence is that their equations of motion, or their Green functions, are altered. This brings gauge covariance into

**Citation:** El-Bennich, B. Gauge covariance of the gap equation. *Symmetry* **2024**, *1*, 0. <https://doi.org/>

Received:

Revised:

Accepted:

Published:

**Copyright:** © 2024 by the author. Submitted to *Symmetry* for possible open access publication under the terms and conditions of the Creative Commons Attribution (CC BY) license (<https://creativecommons.org/licenses/by/4.0/>).

arXiv:2412.19911v1 [hep-ph] 27 Dec 2024

play, which means that the Green functions are not gauge invariant though they obey well-defined transformations with respect to the local gauge group. How these Green functions specifically transform under gauge variation is described by the Landau-Khalatnikov-Fradkin transformations (LKFT) [6,7] within the class of linear covariant gauges. If these transformations are correctly applied, physical observables derived from Green functions in any given gauge should be *identical*. This is exactly what we call gauge invariance. We recall that the Nielsen identities also provide a means to relate variations of Green functions under a gauge parameter change [8,9].

In practice, the application of the LFKT is rather cumbersome, as they are written in coordinate space. One must first obtain a nonperturbative solution for a given Green function in a given gauge, for instance the quark propagator in Landau gauge, and then Fourier transform it to coordinate space. After this one applies the LFKT and Fourier transforms this gauge-transformed propagator back to the momentum space for any arbitrary covariant gauge. However, since the LFKT are nonperturbative in nature, the initial propagator should also be the solution of the nonperturbative gap equation. The latter is described by a Dyson-Schwinger equation (DSE) which involves, besides the boson and fermion propagators, the fully-dressed fermion-boson vertex. The LFKT themselves do not tell us anything about the general form of this vertex, but we can make use of the WGTI identity in QED or of the Slavnov-Taylor identity in QCD [10,11] to constrain at least its non-transverse parts, and also of transverse WGTIs [12–16] and STIs [17] to deduce the transverse vertices [18–20].

This is an arduous and nontrivial task and the procedure has been shown to be feasible with analytical expressions in leading truncation schemes in QED [21]. In an  $SU(N)$  gauge field theory and for covariant  $R_\zeta$  gauges, the transformation law for the quark propagator was derived with a perturbative expansion of the  $SU(N)$  gauge transformation of the quark field to  $\mathcal{O}(g_s^6)$  in the corresponding two-point Green function [22]. Another derivation of the LFKT in non-Abelian theories was given in Ref. [23].

Recently, an alternative path was taken comparing the solutions of the quark DSE in different covariant  $R_\zeta$  gauges [24]. The gauge dependence in this gap equation is twofold, for the dependence on  $\zeta$  enters directly via the gluon dressing function in  $R_\zeta$  gauges, obtained in lattice QCD simulations [25] up to  $\zeta = 0.5$ , and the strong coupling  $\alpha_s^\zeta$ . Indirectly, the dressed quark-gluon vertex also contributes to this dependence and this feature will be exploited in the present study. The numerical data of the  $\zeta$ -dependent gluon propagators was fitted with a Padé approximant which revealed that the fit parameters exhibit a nearly linear dependence on the gauge parameter. This feature was taken advantage of and the gluon propagator was then extrapolated to Feynman gauge. Employing the full quark-gluon vertex derived from Slavnov-Taylor identities and gauge covariance in Ref. [19], the quark's mass and wave renormalization functions were computed in the range  $\zeta \in [0, 1]$ . The quark condensate derived therefrom exhibits a modest dependence on the gauge parameter within the error estimates of the lattice predictions for the gluon, in agreement with a prediction of the LKFT in QCD [22].

We here take the opportunity to extend the study of Ref. [24] by including simpler truncations of the DSE for comparison and to highlight their effect on the gauge covariance of the gap equation. As we shall see, the functional  $\zeta$ -dependence of the quark-mass function is diametrically opposed when the DSE is solved in either the rainbow truncation or with the full vertex structure. Moreover, the quark condensate and pion decay constant, the gauge-parameter dependence of the latter presented here for the first time, decrease as functions of  $\zeta$  in this leading truncation scheme, in disagreement with the gauge-invariance predictions of the LFKT. To a certain extent this is expected, as the rainbow-ladder truncation badly violates the WGTI and STI and is therefore commonly employed in Landau gauge to “minimize” the error. Nonetheless, we here explicitly demonstrate the failure of a simpler truncation to satisfy gauge covariance.

## 2. Quark gap equation: truncation schemes

In QCD, two-point Green functions, in particular the nonperturbative dressing of a current quark, are described by DSEs which are the relativistic equations of motion in that theory [1]. For arbitrary gauge and written in Euclidean space, the DSE of the quark propagator is given by:

$$S_{\xi}^{-1}(p) = Z_2 i \gamma \cdot p + Z_4 m(\mu) + Z_1 4\pi\alpha_s^{\xi} \int^{\Lambda} \frac{d^4k}{(2\pi)^4} \Delta_{\mu\nu}^{ab}(q) \gamma_{\mu} t^a S_{\xi}(k) \Gamma_{\nu}^{b\xi}(k, p). \quad (1)$$

\* In this DSE,  $Z_1(\mu, \Lambda)$ ,  $Z_2(\mu, \Lambda)$  and  $Z_4(\mu, \Lambda)$  are the vertex, wave function and mass renormalization constants, respectively, and  $m(\mu)$  is the renormalized current-quark mass. In the self-energy integral,  $\Lambda$  is a Poincaré-invariant cut-off, whereas  $\mu$  is the renormalization point chosen such that  $\Lambda \gg \mu$ .

The quark-gluon interaction is described by the dressed vertex  $\Gamma_{\mu}^{a\xi}(k, p) = \Gamma_{\mu}^{\xi}(k, p) t^a$ , where  $t^a = \lambda^a/2$  are the  $SU(3)_c$  group generators in the fundamental representation,  $p$  is the incoming quark momentum,  $k$  is the outgoing momentum and  $q = k - p$  is the gluon momentum. The gluon propagator in  $R_{\xi}$  gauge,

$$\Delta_{\mu\nu}^{ab}(q) = \delta^{ab} \left( \delta_{\mu\nu} - \frac{q_{\mu} q_{\nu}}{q^2} \right) \Delta_{\xi}(q^2) + \delta^{ab} \xi \frac{q_{\mu} q_{\nu}}{q^4}, \quad (2)$$

is characterized by a transverse dressing function, renormalized as  $\Delta_{\xi}(\mu^2) = 1/\mu^2$ . The gauge-parameter dependence of this dressing function has been studied with lattice-QCD and functional approaches [25–27].

The covariant decomposition of the DSE solutions is generally written in terms of two amplitudes, namely  $A_{\xi}(p^2)$  and  $B_{\xi}(p^2)$ ,

$$S_{\xi}(p) = \frac{1}{i\gamma \cdot p A_{\xi}(p^2) + B_{\xi}(p^2)} = \frac{Z_{\xi}(p^2)}{i\gamma \cdot p + M_{\xi}(p^2)} = -i\gamma \cdot p \sigma_{\xi}^{\xi}(p^2) + \sigma_{\xi}^{\xi}(p^2), \quad (3)$$

where the flavor- and gauge-dependent mass and wave renormalization functions can be expressed by the two momentum dependent amplitudes:

$$M_{\xi}(p^2) = B_{\xi}(p^2, \mu^2)/A_{\xi}(p^2, \mu^2), \quad Z_{\xi}(p^2, \mu^2) = 1/A_{\xi}(p^2, \mu^2). \quad (4)$$

The renormalization scale we employ is low,  $\mu = 4.3$  GeV, as it is the scale at which the transverse dressing function  $\Delta_{\xi}(q^2)$  in  $R_{\xi}$  gauge is renormalized [25] and allows for comparison of  $M_{\xi}(p^2)$  and  $Z_{\xi}(p^2, \Lambda^2)$  with lattice QCD at this scale [28]. We therefore also impose the following conditions:  $Z_{\xi}(\mu^2) = 1$  and  $M_{\xi}(\mu^2) \equiv m(\mu^2) = 25$  MeV [29–31].

Coming back to the quark-gluon vertex introduced in Eq. (1), its most general covariant decomposition is not unique. For all that, one can express this vertex most generally as [32],

$$\Gamma_{\mu}^{\xi}(k, p) = \Gamma_{\mu}^{L\xi}(k, p) + \Gamma_{\mu}^{T\xi}(k, p) = \sum_{i=1}^4 \lambda_i^{\xi}(k, p) L_{\mu}^i(k, p) + \sum_{i=1}^8 \tau_i^{\xi}(k, p) T_{\mu}^i(k, p), \quad (5)$$

where we stress the gauge dependence of the so-called longitudinal and transverse form factors,  $\lambda_i^{\xi}(k, p)$  and  $\tau_i^{\xi}(k, p)$ , respectively. The transverse vertex is naturally defined by  $iq \cdot \Gamma^{T\xi}(k, p) = 0$ . The 12 vector structures  $L_{\mu}^i(k, p)$  and  $T_{\mu}^i(k, p)$  are build upon the three available vectors, namely  $\gamma_{\mu}$ ,  $k_{\mu}$  and  $p_{\mu}$  and variations thereof, with the constraint that  $\Gamma_{\mu}^{\xi}(k, p)$  should exhibit the same transformation properties as the bare vertex  $\gamma_{\mu}$  under charge conjugation  $C$ , parity transformation  $P$  and time reversal  $T$ .

In Section 3 we will observe the impact of a given truncation of Eq. (1) on gauge covariance. To this end, we consider three cases, namely the leading rainbow truncation, a ghost-corrected Ball-Chiu vertex that satisfies the “longitudinal” STI [29,33,34], and the full longitudinal and transverse vertex structure derived with an additional transverse

STI [19,20]. In the following, we present the form factors  $\lambda_i^\xi(k, p)$  and  $\tau_i^\xi(k, p)$  considered in each case, while the common basis elements  $L_\mu^i(k, p)$  and  $T_\mu^i(k, p)$  are listed in the Appendix.

Rainbow truncation:

$\Gamma_\mu^\xi(k, p) = \gamma_\mu$ ; the bare vertex, successfully employed with phenomenological interaction models to describe light hadrons [35] carries neither dynamical nor gauge information:  $\lambda_1^\xi(k, p) = 1$ ,  $\lambda_{2,3,4}^\xi(k, p) = \tau_{1-8}^\xi(k, p) = 0$ . This truncation is commonly employed with an interaction model or an artificially scaled-up strong coupling to compensate for the lack of support in the DSE kernel [31,36]. Simple extensions include a flavor dependent coupling in the treatment of heavy-light mesons and heavy quarkonia [37–41].

STI Ball-Chiu vertex:

$\Gamma_\mu^\xi(k, p) = \sum_{i=1}^4 \lambda_i^\xi(k, p) L_\mu^i(k, p)$ ; this vertex is constructed to satisfy the STI, however the quark-ghost scattering amplitude that enters this identity is modeled in a dressed-propagator approach and only the leading form factor  $X_0^\xi(k, p)$  is kept; see Refs. [29,33,34,42] for details.

$$\lambda_1^\xi(k, p) = \frac{1}{2} G(q^2) X_0^\xi(q^2) \left[ A_\xi(k^2) + A_\xi(p^2) \right], \quad (6)$$

$$\lambda_2^\xi(k, p) = G(q^2) X_0^\xi(q^2) \frac{A_\xi(k^2) - A_\xi(p^2)}{k^2 - p^2}, \quad (7)$$

$$\lambda_3^\xi(k, p) = G(q^2) X_0^\xi(q^2) \frac{B_\xi(k^2) - B_\xi(p^2)}{k^2 - p^2}, \quad (8)$$

$$\lambda_4^\xi(k, p) = 0. \quad (9)$$

The dressing function  $G(q^2)$  we use [43] is defined by the ghost propagator  $D^{ab}(q^2) = -\delta^{ab} G(q^2)/q^2$  and renormalized as  $G(4.3^2 \text{ GeV}^2) = 1$ . Moreover,  $\tau_1^\xi(k, p) = \tau_2^\xi(k, p) = \dots = \tau_8^\xi(k, p) = 0$ .

Full STI vertex:

$\Gamma_\mu^\xi(k, p) = \sum_{i=1}^4 \lambda_i^\xi(k, p) L_\mu^i(k, p) + \sum_{i=1}^8 \tau_i^\xi(k, p) T_\mu^i(k, p)$ ; the transverse STI constrains the vector structures transverse to the gluon momentum and in addition to the vertex components, Eqs. (6) to (9), one finds with the same approximation for the quark-ghost kernel [19] the following transverse form factors:

$$\tau_1^\xi(k, p) = -\frac{Y_1}{2(k^2 - p^2)\nabla(k, p)}, \quad (10)$$

$$\tau_2^\xi(k, p) = -\frac{Y_5 - 3Y_3}{4(k^2 - p^2)\nabla(k, p)}, \quad (11)$$

$$\tau_3^\xi(k, p) = \frac{1}{2} G(q^2) X_0^\xi(q^2) \left[ \frac{A_\xi(k^2) - A_\xi(p^2)}{k^2 - p^2} \right] + \frac{Y_2}{4\nabla(k, p)} - \frac{t^2(Y_3 - Y_5)}{8(k^2 - p^2)\nabla(k, p)}, \quad (12)$$

$$\tau_4^\xi(k, p) = -\frac{6Y_4 + Y_6^A}{8\nabla(k, p)} - \frac{t^2 Y_7^S}{8(k^2 - p^2)\nabla(k, p)}, \quad (13)$$

$$\tau_5^\xi(k, p) = -G(q^2) X_0^\xi(q^2) \left[ \frac{B_\xi(k^2) - B_\xi(p^2)}{k^2 - p^2} \right] - \frac{2Y_4 + Y_6^A}{2(k^2 - p^2)}, \quad (14)$$

$$\tau_6^\xi(k, p) = \frac{(k-p)^2 Y_2}{4(k^2 - p^2)\nabla(k, p)} - \frac{Y_3 - Y_5}{8\nabla(k, p)}, \quad (15)$$

$$\tau_7^\xi(k, p) = \frac{q^2(6Y_4 + Y_6^A)}{4(k^2 - p^2)\nabla(k, p)} + \frac{Y_7^S}{4\nabla(k, p)}, \quad (16)$$

$$\tau_8^\xi(k, p) = -G(q^2)X_0^\xi(q^2) \left[ \frac{A_\xi(k^2) - A_\xi(p^2)}{k^2 - p^2} \right] - \frac{2Y_8^A}{k^2 - p^2}, \quad (17)$$

where  $Y_i \equiv Y_i^\xi(k, p)$  and the Gram determinant is defined by:  $\nabla(k, p) = k^2 p^2 - (k \cdot p)^2$ . In Eqs. (10) to (17), the  $Y_i^{(A,S)}$  functions are the form factors of the most general decomposition of a Fourier transformed four-point function in coordinate space. The latter involves a non-local vector vertex along with a Wilson line to preserve gauge invariance and contributes to the transverse STI. Since we deal with a rather complex object for which no calculations exist yet, we refer to the discussion in Ref. [17] and note that the  $Y_i^{(A,S)}$  were constrained [18] with a vertex ansatz guided by pQCD and multiplicative renormalizability [44]. We do stress the fact, however, that the functions  $Y_1(k, p)$ ,  $Y_6^A(k, p)$  and  $Y_7^S$  are *massive*, i.e. they are proportional to the mass function  $B(k^2)$ . The contribution to DCSB of the vertex form factors in Eqs. (6) to (17) that depend directly on  $B(k^2)$  or indirectly via these functions is therefore crucial and we observe that no mass function solutions are found if all  $Y_i(k, p)$  are zero, regardless of the value of the strong coupling  $\alpha_s(\mu)$ . The same occurs if one chooses  $\tau_4(k, p) = \tau_7(k, p) = 0$ . Indeed, these two transverse form factors are responsible for the overwhelming contribution to DCSB in the gap equation [19].

The gauge dependence of the strong coupling has been studied with the Schwinger mechanism in the three-gluon vertex that is crucial to a gluon-mass generation in the infrared domain [45],

$$\alpha_s^\xi = \alpha_s^0 + 0.098\xi - 0.064\xi^2. \quad (18)$$

where we use  $\alpha_s^0 = 0.29$  for the ghost-corrected Ball-Chiu and the full STI vertices at  $\mu = 4.3$  GeV. On the other hand, solving the DSE with such a small coupling in the rainbow truncation leads to a very modest mass generation,  $M_\xi^{u,d}(0) \approx 70$  MeV. In analogy with effective interaction models we therefore inflate the coupling strength and choose  $\alpha_s^0 = 1.0$ , which results in a constituent mass of the same order than that found with the full STI vertex.

### 3. Gauge dependence of the mass and wave renormalization

We now discuss the solutions,  $M_\xi(p^2)$  and  $Z_\xi(p^2)$ , of Eq. (1) for the three cases considered in Section 2. Henceforth, we make use of the gluon and ghost dressing functions from lattice QCD,  $\Delta_\xi(q^2)$  [25] and  $G(q^2)$  [43] respectively, renormalized at  $\mu = 4.3$  GeV and parametrized with a Padé approximant [46]:

$$\Delta_\xi(q^2) = Z \frac{q^2 + M_1^2}{q^4 + M_2^2 q^2 + M_3^4} \left[ 1 + \omega \ln \left( \frac{q^2 + M_0^2}{\Lambda_{\text{QCD}}^2} \right) \right]^{\gamma_{\text{gl}}}, \quad (19)$$

where  $\omega = 11N_c \alpha_s(\mu)/12\pi$ ,  $\Lambda_{\text{QCD}} = 0.425$  GeV and  $\gamma_{\text{gl}} = (13 - 3\xi)/22$  is the 1-loop anomalous gluon dimension. This parametrization is tantamount to a renormalization-group improved Padé approximation and is motivated by the refined Gribov-Zwanziger tree-level gluon propagator in the infrared region. The parameters  $Z$ ,  $M_0$ ,  $M_1$ ,  $M_2$  and  $M_3$  were determined in a least- $\chi^2$  fit in Ref. [24] and exhibit a *nearly* linear dependence on the gauge parameter  $\xi$  when fitted to the lattice data for the six values,  $\xi = 0, 0.1, 0.2, 0.3, 0.4, 0.5$ . This feature was used to extrapolate the gluon propagator up to Feynman gauge [24].

The ghost propagator [43] is parametrized with a similar expression,

$$G(q^2) = Z \frac{q^4 + M_2^2 q^2 + M_1^4}{q^4 + M_4^2 q^2 + M_3^4} \left[ 1 + \omega \ln \left( \frac{q^2 + \frac{m_1^4}{q^2 + m_0^2}}{\Lambda_{\text{QCD}}^2} \right) \right]^{\gamma_{\text{gh}}}, \quad (20)$$

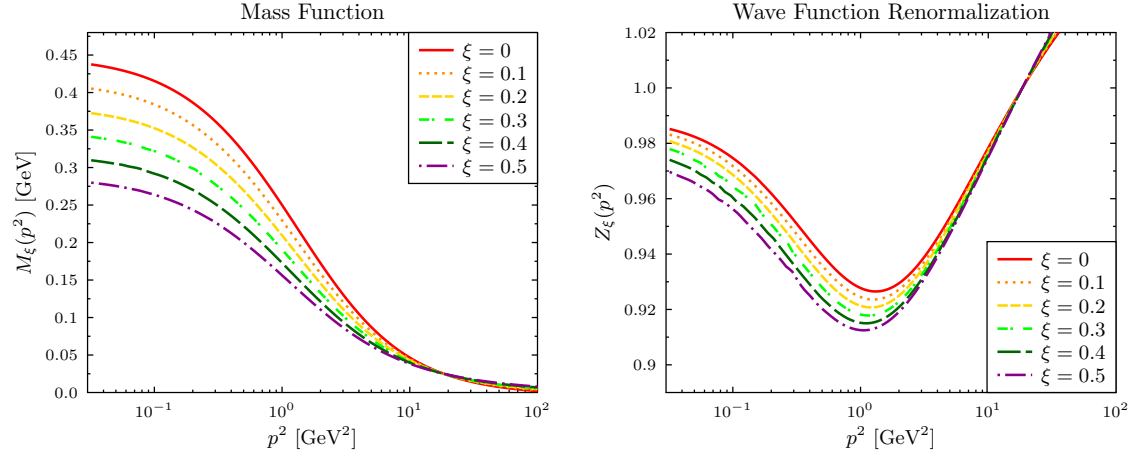


**Figure 1.** Gauge-parameter dependence of the  $M_{\xi}(p^2)$  and  $Z_{\xi}(p^2)$  functions of light quarks ( $m_u = m_d$ ) in the rainbow truncation of the DSE. Note that the strong coupling has been artificially inflated to  $\alpha_s^0 = 1.17$ .

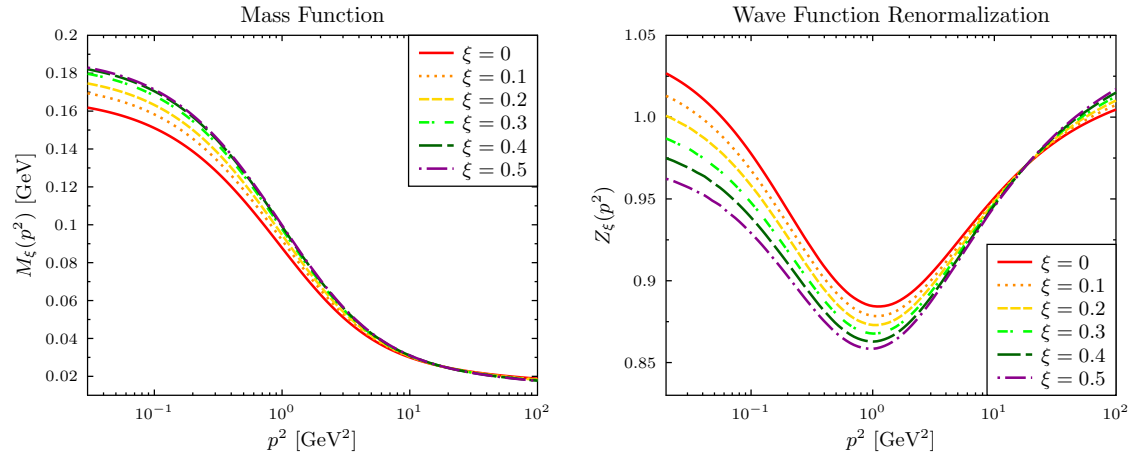


**Figure 2.** The gauge-parameter dependence of  $M_{\xi}(p^2)$  and  $Z_{\xi}(p^2)$  of the light quark employing the STI Ball-Chiu vertex, Eqs. (6) to (9), in the DSE (1).

and is assumed to be independent of  $\zeta$  [47]. The anomalous ghost dimension is given by  $\gamma_{\text{gh}} = -9/44$  and  $\omega$ ,  $\Lambda_{\text{QCD}}$  and  $\mu$  are as in Eq. (19). The fit parameters are also found in Ref. [24].

In Fig. 1 we plot the mass and wave-renormalization functions and their gauge-parameter dependence for the bare vertex. As mentioned earlier, with  $\alpha_s^0 \approx 0.3$  the dynamical mass generation is insufficient to produce a true constituent-quark mass in any gauge. Hence, we inflate the constant to  $\alpha_s^0 = 1.0$ , as this will allow us to compare quark condensates and weak decay constants obtained with the full STI vertex later on. The gauge dependence of  $M_{\xi}(p^2)$  is pronounced and the mass steadily decreases as a function of the gauge parameter. This behavior was also observed in mass and wave-renormalization functions solving the DSE in quenched QED3 with  $\Gamma_{\mu}^{\xi}(k, p) = \gamma_{\mu}$  [21]. Likewise,  $Z_{\xi}(p^2)$  also decreases as a function of  $\xi$  in the range considered here.

Solving the DSE (1) with the non-transverse vertex defined by Eqs. (6) to (9), we obtain the mass and wave-renormalization functions of Fig. 2. We observe that the gauge dependence of the gap equation leads to a behavior of  $M_{\xi}(p^2)$  opposed to that in Fig. 1: the effect of the additional gauge dependence in the vertex is an increase of  $M_{\xi}(p^2)$  up to  $\xi = 0.5$ , at which point the function seemingly freezes. The functional behavior of  $Z_{\xi}(p^2)$  exhibits the characteristic behavior of the Ball-Chiu vertex, with a local minimum at  $p \approx 1$  GeV and a sudden rise in the infrared, though the gauge dependence is more

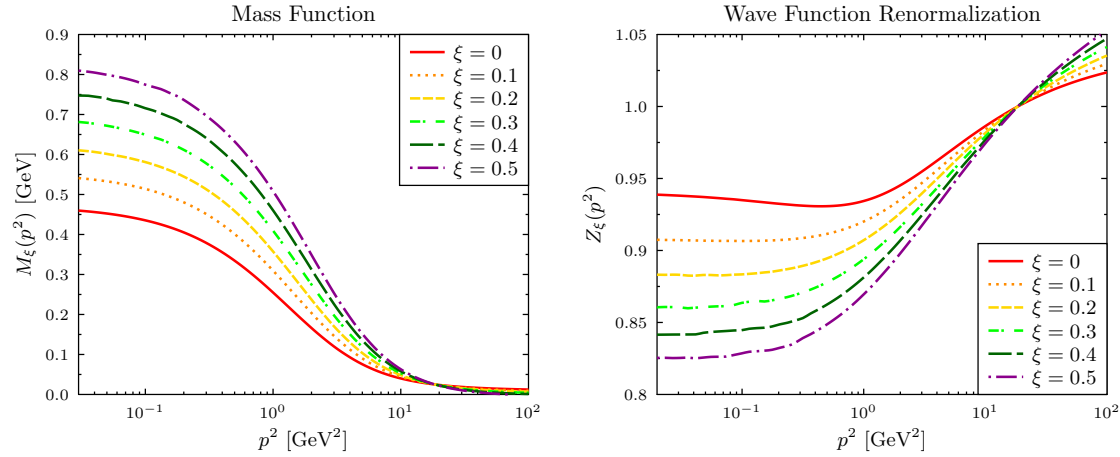


**Figure 3.**  $M_{\xi}(p^2)$  and  $Z_{\xi}(p^2)$  as functions of the gauge parameter  $\xi$  DSE (1) of the light quarks when the DSE (1) is solved with the full STI vertex  $\Gamma_{\mu}^{\xi}(k, p)$ , Eqs. (6) to (17).

perceptible that in the rainbow truncation, Fig. 1. We remark that the solutions of the mass and wave-renormalization functions with the STI Ball-Chiu vertex are increasingly unstable for  $\xi > 0.5$ . We therefore do not include the Feynman gauge solutions in Fig. 2 and for comparison's sake we also restrain from doing so in Figs. 1 and 3.

In Fig. 3 we present our solutions for  $M_{\xi}(p^2)$  and  $Z_{\xi}(p^2)$  with the full, gauge-dependent STI vertex defined by Eqs. (6) to (17). Clearly, the trend of a rising mass function and a dropping wave renormalization in the low-momentum region observed with the ghost-corrected Ball-Chiu vertex is confirmed when the transverse vertex is included. The contrast with the functional behavior in Fig. 1 is evident, in particular that of  $Z_{\xi}(p^2)$  which now decreases steadily with  $\xi$  and saturates in the infrared domain. Moreover, the quark-ghost scattering form factor,  $X_0^{\xi}(k, p)$ , is calculated in a dressed approximation [29,33,34] and

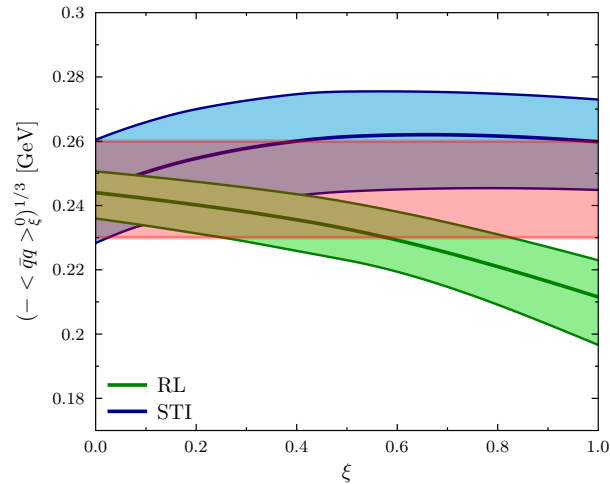


**Figure 4.** Gauge dependence of the chiral quark condensate obtained with two different quark-gluon vertices in the DSE. The pink, green and blue shaded error bands stem from the statistical errors of the lattice QCD predictions for the gluon and ghost propagators [25] on which the gauge-dependent solutions of  $A_{\xi}(p^2)$  and  $B_{\xi}(p^2)$  depend via Eqs. (1) and (2). The pink horizontal band indicates the region of a gauge-independent quark condensate as implied by the LKFT in QCD, where the uncertainty is due to the statistical error of the gauge propagators in Landau gauge.

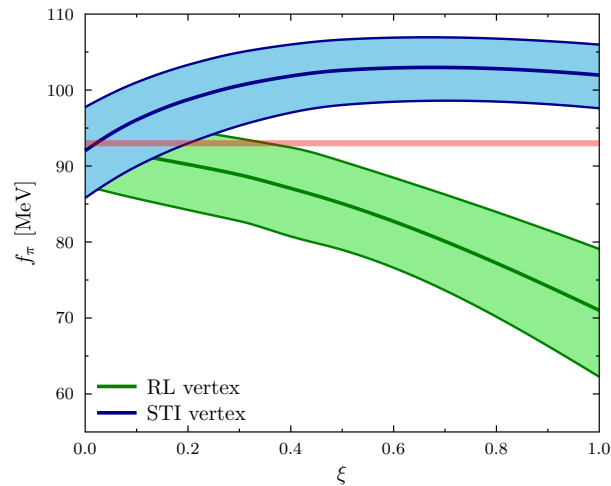


**Figure 5.** Gauge dependence of the pion decay constant for two different quark-gluon vertices in the DSE (1). The error estimate represented by the green and blue bands is as in Fig. 4, while the horizontal pink line represents the experimental reference value.

dynamically generated in consistency with  $M_\zeta(p^2)$  and  $Z_\zeta(p^2)$ . We abstain from discussing the gauge-dependent solutions here and refer to Ref. [24] for details.

To conclude our comparison of gauge dependent quark propagators, we ought to ask which is the correct one. This question can only be answered by computing a gauge-invariant quantity with the given quark propagators. A simple quantity that does not require the solutions of a Bethe-Salpeter equation is the quark condensate in the chiral limit ( $\Lambda = 1$  GeV),

$$-\langle \bar{q}q \rangle_\zeta^0 \equiv Z_4 N_c \int \frac{d^4 k}{(2\pi)^4} \text{tr}_D [S_\zeta^0(k)], \quad (21)$$

which we can express as a function of  $\zeta$ . As can be inferred from Fig. 4, the condensate calculated with the full STI vertex is the central line in the blue-shaded, fairly horizontal band. The latter depicts our error estimate due to the statistical error of the gluon propagator [25]. A systematic error is not included, but we allow for uncertainties of the ghost dressing function and of  $\alpha_s^\zeta$  (18) by varying  $\Delta_\zeta(q^2)$  by  $\pm 5\%$ . In this light, one can argue that the QCD condensate exhibits a moderate dependence on  $\zeta$  of the order of 7–8%, rising initially from Landau gauge to  $\zeta \approx 0.3$  where the condensate seems to level off. This is in accordance with an invariance proof for any  $SU(N)$  theory derived in Ref. [22] and based on the LKFT. The same figure also demonstrates that this is not the case for a quark condensate computed in the rainbow truncation of the DSE. In fact, while an extrapolation beyond  $\zeta = 1.0$  of the gluon propagator must be taken with a grain of salt, we verified that the condensate in this simplest truncation keeps falling off with the gauge parameter. This functional behavior expresses the lack of gauge covariance in this leading truncation not constrained by the STI and multiplicative renormalizability.

We can also calculate the weak decay constant of the pion in the chiral limit following Ref. [48], as  $f_\pi$  does not vanish in this limit whereas the pion's mass does in truncations that preserve the axialvector WGTI. The weak decay constant in the chiral limit can be expressed by the integral,

$$\begin{aligned} (f_\pi^0)^2 = \frac{N_c}{8\pi^2} \int_0^\infty dp^2 p^2 B^2(p^2) & \left( \sigma_v^2 - 2 \left[ \sigma_s \sigma'_s + p^2 \sigma_v \sigma'_v \right] \right. \\ & \left. - p^2 \left[ \sigma_s \sigma''_s - (\sigma'_s)^2 \right] - p^4 \left[ \sigma_v \sigma''_v - (\sigma'_v)^2 \right] \right), \end{aligned} \quad (22)$$

with  $\sigma'_{s,v} \equiv d\sigma_{s,v}(p^2)/dp^2$  and where we dropped the gauge dependence label. As we are constrained by a low renormalization point due to the quenched lattice-QCD input for the



gluon and ghost propagators we employ, we set  $m(\mu) = 0$  MeV at  $\mu = 4.3$  GeV, which allows for a sensible approximation for  $\sigma_s(p^2)$  and  $\sigma_v(p^2)$  in Eq. (22).

In analogy with the condensates presented in Fig. 4, the rainbow truncation of the DSE yields a weak decay constant that decreases relatively fast, as can be appreciated in Fig. 5. If we solve the DSE with the full STI vertex, we observe an initial increase of  $f_\pi$  from  $\zeta = 0$  to  $\zeta \approx 0.5$  after which the decay constant appears to saturate. The variation between Landau and Feynman gauge is about 10%, larger than the 6% increase of the quark condensate as function of  $\zeta$ . However, this moderate effect is not yet conclusive as we ought to compute  $f_\pi$  with the complete Bethe-Salpeter amplitude of the pion in this much more challenging truncation.

#### 4. Final remarks

We have shown that within a functional approach to QCD, the transverse quark-gluon vertex plays a major role in the dynamics of mass generation and the emergence of a constituent quark mass scale. Regarding the gauge parameter dependence of the gap equation, we find a running mass function that increases with  $\zeta$  and a quark wave function which is mostly sensible to the gauge parameter in the infrared domain. More precisely,  $Z(0)$  drops from about 0.94 in Landau gauge to 0.83 for  $\zeta = 0.5$ , a 7% effect. As far as gauge invariance is concerned, despite the limitations of the setup used herein, a variation of about 6% is observed in the quark condensate when the full vertex is taken into account in the gap equation. This contrasts with the outcome of the rainbow approximation which yields a condensate that decreases with  $\zeta$ . Likewise,  $f_\pi$  rapidly falls off as a function of the gauge parameter. These results illustrate, once more, the important role of the transverse vertex in the nonperturbative dynamics of the gap equation.

**Funding:** This research was funded by the São Paulo Research Foundation (FAPESP), grant no. 2023/00195-8 and by the National Council for Scientific and Technological Development (CNPq), grant no. 409032/2023-9. B. E. is a member of the Brazilian nuclear physics network project *INCT-Física Nuclear e Aplicações*, grant no. 464898/2014-5.

**Acknowledgments:** Much of what I presented in this contribution has only been possible with the precious input and contributions by Luis Albino, Adnan Bashir, Roberto Correa da Silveira, José Lessa, Orlando Oliveira and Fernando Serna over the past years. I would like to express my gratitude to Kazuo Tsushima, Anthony Thomas and Myung Ki Cheoun for the opportunity to contribute the *Symmetry* special issue *Chiral Symmetry, and Restoration in Nuclear Dense Matter*.

**Conflicts of Interest:** The author declares no conflicts of interest.

#### Abbreviations

The following abbreviations are used in this manuscript:

QCD	Quantum Chromodynamics
QED	Quantum Electrodynamics
DSE	Dyson-Schwinger equation
LFKT	Landau-Khalatnikov-Fradkin transformation
WGTI	Ward-Green-Takahashi identity
STI	Slavnov-Taylor identity

## Appendix A

For the longitudinal vertex we employ the common Ball-Chiu decomposition ( $t = k + p$ ):

$$L_{\mu}^1(k, p) = \gamma_{\mu}, \quad (\text{A1})$$

$$L_{\mu}^2(k, p) = \frac{1}{2} t_{\mu} \gamma \cdot t, \quad (\text{A2})$$

$$L_{\mu}^3(k, p) = -i t_{\mu}, \quad (\text{A3})$$

$$L_{\mu}^4(k, p) = -\sigma_{\mu\nu} t_{\nu}. \quad (\text{A4})$$

The transverse vertex can generally be decomposed into eight independent vector basis elements. For the kinematical configuration discussed below Eq. (1) these are:

$$T_{\mu}^1(k, p) = i[p_{\mu}(k \cdot q) - k_{\mu}(p \cdot q)], \quad (\text{A5})$$

$$T_{\mu}^2(k, p) = [p_{\mu}(k \cdot q) - k_{\mu}(p \cdot q)] \gamma \cdot t, \quad (\text{A6})$$

$$T_{\mu}^3(k, p) = q^2 \gamma_{\mu} - q_{\mu} \gamma \cdot q, \quad (\text{A7})$$

$$T_{\mu}^4(k, p) = iq^2 [\gamma_{\mu} \gamma \cdot t - t_{\mu}] + 2q_{\mu} p_{\nu} k_{\rho} \sigma_{\nu\rho}, \quad (\text{A8})$$

$$T_{\mu}^5(k, p) = \sigma_{\mu\nu} q_{\nu}, \quad (\text{A9})$$

$$T_{\mu}^6(k, p) = -\gamma_{\mu} (k^2 - p^2) + t_{\mu} \gamma \cdot q, \quad (\text{A10})$$

$$T_{\mu}^7(k, p) = \frac{i}{2} (k^2 - p^2) [\gamma_{\mu} \gamma \cdot t - t_{\mu}] + t_{\mu} p_{\nu} k_{\rho} \sigma_{\nu\rho}, \quad (\text{A11})$$

$$T_{\mu}^8(k, p) = -i \gamma_{\mu} p_{\nu} k_{\rho} \sigma_{\nu\rho} - p_{\mu} \gamma \cdot k + k_{\mu} \gamma \cdot p. \quad (\text{A12})$$

We use a slightly modified basis [49] with respect to the Ball-Chiu vertex [32], with the effect that all transverse form factors are independent of kinematic singularities in one-loop perturbation theory with arbitrary covariant gauge.

## References

1. A. Bashir, L. Chang, I. C. Cloët, B. El-Bennich, Y. X. Liu, C. D. Roberts and P. C. Tandy, *Commun. Theor. Phys.* **58** (2012), 79-134 doi:10.1088/0253-6102/58/1/16
2. Y. B. Yang, J. Liang, Y. J. Bi, Y. Chen, T. Draper, K. F. Liu and Z. Liu, *Phys. Rev. Lett.* **121** (2018) no.21, 212001 doi:10.1103/PhysRevLett.121.212001
3. J. C. Ward, *Phys. Rev.* **78** (1950), 182 doi:10.1103/PhysRev.78.182
4. H. S. Green, *Proc. Phys. Soc. A* **66** (1953), 873-880 doi:10.1088/0370-1298/66/10/303
5. Y. Takahashi, *Nuovo Cim.* **6** (1957), 371 doi:10.1007/BF02832514
6. L. D. Landau and I. M. Khalatnikov, *Zh. Eksp. Teor. Fiz.* **29** (1955), 89
7. E. S. Fradkin, *Zh. Eksp. Teor. Fiz.* **29** (1955), 258-261
8. N. K. Nielsen, *Nucl. Phys. B* **101** (1975), 173-188 doi:10.1016/0550-3213(75)90301-6
9. T. De Meerleer, D. Dudal, S. P. Sorella, P. Dall'Olivo and A. Bashir, *Phys. Rev. D* **101** (2020) no.8, 085005 doi:10.1103/PhysRevD.101.085005
10. A. A. Slavnov, *Theor. Math. Phys.* **10** (1972), 99-107 doi:10.1007/BF01090719
11. J. C. Taylor, *Nucl. Phys. B* **33** (1971), 436-444 doi:10.1016/0550-3213(71)90297-5
12. K. I. Kondo, *Int. J. Mod. Phys. A* **12** (1997), 5651-5686 doi:10.1142/S0217751X97002978
13. H. X. He, F. C. Khanna and Y. Takahashi, *Phys. Lett. B* **480** (2000), 222-228 doi:10.1016/S0370-2693(00)00353-1
14. H. X. He, *Commun. Theor. Phys.* **46** (2006), 109-112 doi:10.1088/0253-6102/46/1/025
15. H. X. He, *Int. J. Mod. Phys. A* **22** (2007), 2119-2132 doi:10.1142/S0217751X07036257
16. M. R. Pennington and R. Williams, *J. Phys. G* **32** (2006), 2219-2234 doi:10.1088/0954-3899/32/11/014
17. H. x. He, *Phys. Rev. D* **80** (2009), 016004 doi:10.1103/PhysRevD.80.016004
18. L. Albino, A. Bashir, L. X. G. Guerrero, B. E. Bennich and E. Rojas, *Phys. Rev. D* **100** (2019) no.5, 054028 doi:10.1103/PhysRevD.100.054028
19. L. Albino, A. Bashir, B. El-Bennich, E. Rojas, F. E. Serna and R. C. da Silveira, *JHEP* **11** (2021), 196 doi:10.1007/JHEP11(2021)196
20. B. El-Bennich, F. E. Serna, R. C. da Silveira, L. A. F. Rangel, A. Bashir and E. Rojas, *Rev. Mex. Fis. Suppl.* **3** (2022) no.3, 0308092 doi:10.31349/SuplRevMexFis.3.0308092

21. A. Bashir and A. Raya, Nucl. Phys. B **709** (2005), 307-328 doi:10.1016/j.nuclphysb.2004.12.010
22. M. J. Aslam, A. Bashir and L. X. Gutiérrez-Guerrero, Phys. Rev. D **93** (2016) no.7, 076001 doi:10.1103/PhysRevD.93.076001
23. T. De Meerleer, D. Dudal, S. P. Sorella, P. Dall'Olivo and A. Bashir, Phys. Rev. D **97** (2018) no.7, 074017 doi:10.1103/PhysRevD.97.074017
24. J. R. Lessa, F. E. Serna, B. El-Bennich, A. Bashir and O. Oliveira, Phys. Rev. D **107** (2023) no.7, 074017 doi:10.1103/PhysRevD.107.074017
25. P. Bicudo, D. Binosi, N. Cardoso, O. Oliveira and P. J. Silva, Phys. Rev. D **92** (2015) no.11, 114514 doi:10.1103/PhysRevD.92.114514
26. M. Q. Huber, Phys. Rev. D **91** (2015) no.8, 085018 doi:10.1103/PhysRevD.91.085018
27. M. Napetschnig, R. Alkofer, M. Q. Huber and J. M. Pawłowski, Phys. Rev. D **104** (2021) no.5, 054003 doi:10.1103/PhysRevD.104.054003
28. O. Oliveira, P. J. Silva, J. I. Skullerud and A. Sternbeck, Phys. Rev. D **99** (2019) no.9, 094506 doi:10.1103/PhysRevD.99.094506
29. E. Rojas, J. P. B. C. de Melo, B. El-Bennich, O. Oliveira and T. Frederico, JHEP **10** (2013), 193 doi:10.1007/JHEP10(2013)193
30. E. Rojas, B. El-Bennich, J. P. B. C. De Melo and M. A. Paracha, Few Body Syst. **56** (2015) no.6-9, 639-644 doi:10.1007/s00601-015-1020-x
31. F. E. Serna, C. Chen and B. El-Bennich, Phys. Rev. D **99** (2019) no.9, 094027 doi:10.1103/PhysRevD.99.094027
32. J. S. Ball and T. W. Chiu, Phys. Rev. D **22** (1980), 2542 doi:10.1103/PhysRevD.22.2542
33. A. C. Aguilar and J. Papavassiliou, Phys. Rev. D **83**, 014013 (2011) doi:10.1103/PhysRevD.83.014013
34. A. C. Aguilar, J. C. Cardona, M. N. Ferreira and J. Papavassiliou, Phys. Rev. D **96**, no.1, 014029 (2017) doi:10.1103/PhysRevD.96.014029
35. L. Chang, I. C. Cloët, B. El-Bennich, T. Klähn and C. D. Roberts, Chin. Phys. C **33** (2009), 1189-1196 doi:10.1088/1674-1137/33/12/022
36. B. El-Bennich, G. Krein, E. Rojas and F. E. Serna, Few Body Syst. **57** (2016) no.10, 955-963 doi:10.1007/s00601-016-1133-x
37. F. E. Serna, B. El-Bennich and G. Krein, Phys. Rev. D **96** (2017) no.1, 014013 doi:10.1103/PhysRevD.96.014013
38. F. E. Serna, R. C. da Silveira, J. J. Cobos-Martínez, B. El-Bennich and E. Rojas, Eur. Phys. J. C **80** (2020) no.10, 955 doi:10.1140/epjc/s10052-020-08517-3
39. F. E. Serna, R. C. da Silveira and B. El-Bennich, Phys. Rev. D **106**, no.9, L091504 (2022) doi:10.1103/PhysRevD.106.L091504
40. R. C. da Silveira, F. E. Serna and B. El-Bennich, Phys. Rev. D **107**, no.3, 034021 (2023) doi:10.1103/PhysRevD.107.034021
41. F. E. Serna, B. El-Bennich and G. Krein, Phys. Rev. D **110**, no.11, 114033 (2024) doi:10.1103/PhysRevD.110.114033
42. A. I. Davydychev, P. Osland and L. Saks, Phys. Rev. D **63** (2001), 014022 doi:10.1103/PhysRevD.63.014022
43. A. G. Duarte, O. Oliveira and P. J. Silva, Phys. Rev. D **94** (2016) no.1, 014502 doi:10.1103/PhysRevD.94.014502
44. A. Bashir, R. Bermúdez, L. Chang and C. D. Roberts, Phys. Rev. C **85** (2012), 045205 doi:10.1103/PhysRevC.85.045205
45. A. C. Aguilar, D. Binosi and J. Papavassiliou, Phys. Rev. D **95** (2017) no.3, 034017 doi:10.1103/PhysRevD.95.034017
46. D. Dudal, O. Oliveira and P. J. Silva, Annals Phys. **397** (2018), 351-364 doi:10.1016/j.aop.2018.08.019
47. A. Cucchieri, D. Dudal, T. Mendes, O. Oliveira, M. Roelfs and P. J. Silva, PoS **LATTICE2018** (2018), 252 doi:10.22323/1.334.0252
48. C. D. Roberts, Nucl. Phys. A **605**, 475-495 (1996) doi:10.1016/0375-9474(96)00174-1
49. A. Kızılersü, M. Reenders and M. R. Pennington, Phys. Rev. D **52** (1995), 1242-1259 doi:10.1103/PhysRevD.52.1242

**Disclaimer/Publisher's Note:** The statements, opinions and data contained in all publications are solely those of the individual author(s) and contributor(s) and not of MDPI and/or the editor(s). MDPI and/or the editor(s) disclaim responsibility for any injury to people or property resulting from any ideas, methods, instructions or products referred to in the content.